

Effects of molecular rotation in low-energy electron collisions of H_3^+

BY ANDREAS WOLF^{1,*}, H. KRECKEL¹, L. LAMMICH¹, D. STRASSER^{2,†},
J. MIKOSCH^{1,3}, J. GLOSÍK⁴, R. PLAŠIL⁴, S. ALTEVOGT¹,
V. ANDRIANARIJAONA^{1,‡}, H. BUHR¹, J. HOFFMANN¹, M. LESTINSKY¹,
I. NEVO², S. NOVOTNY¹, D. A. ORLOV¹, H. B. PEDERSEN¹,
A. S. TEREKHOV⁵, J. TOKER², R. WESTER³, D. GERLICH⁶,
D. SCHWALM¹ AND D. ZAJFMAN^{1,2}

¹*Max-Planck-Institut für Kernphysik, 69117 Heidelberg, Germany*

²*Department of Particle Physics, Weizmann Institute of Science, Rehovot 76100, Israel*

³*Physikalisches Institut, Universität Freiburg, 79104 Freiburg, Germany*

⁴*Faculty of Mathematics and Physics, Charles University Prague, V Holesovickách 2, 180 00 Prague, Czech Republic*

⁵*Institute of Semiconductor Physics, 630090 Novosibirsk, Russia*

⁶*Institut für Physik, Technische Universität, 09107 Chemnitz, Germany*

Measurements on the energetic structure of the dissociative recombination rate coefficient in the millielectronvolt range are described for H_3^+ ions produced in the lowest rotational levels by collisional cooling and stored as a fast beam in the magnetic storage ring TSR (Test Storage Ring). The observed resonant structure is consistent with that found previously at the storage ring facility CRYRING in Stockholm, Sweden; theoretical predictions yield good agreement on the overall size of the rate coefficient, but do not reproduce the detailed structure. First studies on the nuclear spin symmetry influencing the lowest level populations show a small effect different from the theoretical predictions. Heating processes in the residual gas and by collisions with energetic electrons, as well as cooling owing to interaction with cold electrons, were observed in long-time storage experiments, using the low-energy dissociative recombination rate coefficient as a probe, and their consistency with the recent cold H_3^+ measurements is discussed.

Keywords: dissociative recombination; low-energy resonances;
collisional heating and cooling of rotations

1. Introduction

Collisions of H_3^+ with electrons at a few millielectronvolt energies play a crucial role in cold ionized hydrogen-dominated media (LePetit *et al.* 2004), where this

* Author for correspondence (a.wolf@mpi-hd.mpg.de).

† Present address: Department of Chemistry, University of California, Berkeley, CA 94720-1460, USA.

‡ Present address: Department of Physics and Astronomy, University of Nebraska-Lincoln, Lincoln, NE 68588-0111, USA.

One contribution of 26 to a Discussion Meeting Issue ‘Physics, chemistry and astronomy of H_3^+ ’.

species is a key molecular ion. Exothermic processes, especially dissociative recombination (DR), proceed at arbitrarily low energies of the incident electron through the attractive Coulomb potential of the ion. This way, DR becomes the dominant loss process that determines the H_3^+ concentration (LePetit *et al.* 2004). In addition, exothermic electron collisions with excited H_3^+ ions can lead to internal cooling of the ions, leaving the degree of ionization unchanged (superelastic collisions, SEC; Ngassam *et al.* 2003); similarly, rotational and vibrational electron-impact excitation (EIE; Faure & Tennyson 2003) can also occur. Experimental methods are being continuously improved to investigate these processes in the laboratory at high-electron-energy resolution and for specific rovibrational states.

The understanding from recent theoretical (Kokoouline & Greene 2003) and experimental work (McCall *et al.* 2003) indicates that the rovibrational motion of the three nuclei in the system is strongly involved in the dynamics of the low-energy electron collision processes. In particular, a dominant role is played by resonances where the incident electron is captured in an intermediate neutral H_3 complex by giving up energy to the rovibrational nuclear degrees of freedom. Therefore, the electron collision cross-sections show a distinct energetic structure linked to the positions, strengths, widths and interferences of autoionizing electronic H_3 Rydberg states with a rovibrationally excited H_3^+ core. As each capture resonance can cause DR, SEC or EIE through its various dissociating or autoionizing decay channels, these three processes are strongly linked to each other. Moreover, for reliable predictions of the size and the energy variation of these cross-sections, the resonant structure must be calculated very accurately, especially in the low-energy limit. In fact, large differences in the low-temperature rate coefficients can result from the parameters of individual near-zero energy resonances specific to the various initial rotational states of H_3^+ .

Energy-resolved stored ion experiments detect and analyse the products of single collision events and use a variety of preparation techniques for the initial ion states, which gives them a large potential to unravel the properties and the underlying dynamics of these processes. We here report experiments using long-time stored H_3^+ ions in a magnetic storage ring, employing co-propagating cold electron beams and suitable detectors that yield energy-resolved cross-sections, as well as techniques for defining and modifying the initial rovibrational states in the stored ion beam. The present paper reviews the studies at the magnetic ion storage ring TSR (Test Storage Ring), with particular emphasis on the energy-resolved DR cross-sections and the temporal changes in the low-energy DR rate as a probe for changes of the internal excitation during the long-time storage of H_3^+ ions.

2. Experimental approach

(a) Basic set-up and observations

In the approach followed here, an H_3^+ ion beam is formed by a radiofrequency (RF) high-energy accelerator at an energy of 5.3 MeV, high enough to ensure average storage times of many seconds for the ions in a magnetic storage ring at a vacuum of $ca\ 3 \times 10^{-11}$ mbar. The arrangement of the storage-ring facility TSR (Jaeschke *et al.* 1990) at the Max-Planck Institute of Nuclear Physics in Heidelberg, Germany, is shown in figure 1. Information on ion storage-ring

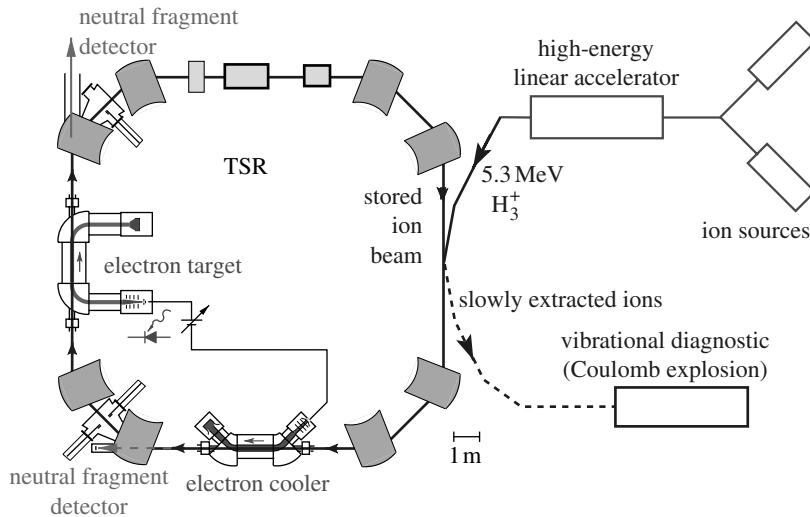


Figure 1. Overview of the Heidelberg TSR facility used for experiments with a stored 5.3 MeV H_3^+ ion beam, showing the ion acceleration scheme, the magnetic deflection structure, the two co-propagating electron beam devices serving as electron cooler (fixed electron velocity) and electron target (variable electron velocity), the neutral fragment extensions for counting and analysing DR processes, as well as the extraction beam line used in separate experiments for time-dependent Coulomb-explosion measurements of the vibrational H_3^+ excitation.

facilities and electron cooling can be found in the literature (e.g. Poth 1990; Wolf 1999; Wolf *et al.* 2004); storage-ring studies of DR were reviewed by Larsson (1997, 2000).

Dissociative recombination measurements are performed after loading ions into the ring, where they circulate freely as a continuous (unbunched) beam. The electron cooler supplies a co-propagating electron beam with a velocity matched to that of the injected ions and, after a precooling period of *ca* 2 s following the injection, the electron cooling process defines the exact ion beam velocity. In a DR measurement using the electron cooler alone, the beam velocity is then detuned for certain time intervals (usually fractions of a second) by changing the electron acceleration voltage (see Al-Khalili *et al.* 2002 for the procedures at the different facilities). While the ions essentially keep the velocity imposed on them by the previous cooling, the DR rate prevailing at the applied average longitudinal velocity detuning between the two beams is measured, using solid-state detectors with nearly unity efficiency to intersect the neutral products just outside the ring. After normalization, the result is given as the DR rate coefficient as a function of the detuning energy E_d of the electrons, obtained from the longitudinal velocity difference, and represents an average over the electron velocity distribution becoming near-monochromatic at sufficiently high E_d (Al-Khalili *et al.* 2002). This distribution is described by the electron temperature in the co-moving reference frame of the electron beam, which assumes different values in longitudinal (T_{\parallel}) and transverse (T_{\perp}) directions. For the electron cooler, values of $kT_{\perp} = 5\text{--}14$ meV and $kT_{\parallel} \sim 0.06$ meV are typical. In this arrangement, using $E_d = 0$, fragment imaging measurements were performed at the TSR that revealed the momentum correlation between the atomic hydrogen atoms in the three-body DR channel of H_3^+ (Strasser *et al.* 2001) and D_3^+ (Strasser *et al.* 2002b)

and of the isotopic analogues D_2H^+ and H^2D^+ (Strasser *et al.* 2004), as well as the rovibrational excitation of the H_2 products in the two-body DR channel of H_3^+ and D_3^+ (Strasser *et al.* 2001, 2002*a,b*).

The electron target (figure 1) is a new device (Sprenger *et al.* 2004) added to the TSR in 2003. Here, a detuned electron beam can be applied while the stored ions are continuously cooled and kept at a given beam velocity by the electron cooler, simultaneously operating at matched velocity. This stabilizes and improves the ion beam quality of electron collision measurements and offers new experimental possibilities, such as the pump-probe operation discussed below. New counting and fragment imaging detectors are applied together with the electron target. For small velocity detunings (as in molecular studies), a direct electrical interconnection between the electron sources in the cooler and the target increases the precision, in which only a small, well-controlled potential difference is applied to define the velocity detuning. Electron temperatures typically achieved in the electron target with a thermal cathode are $kT_{\perp} \sim 4$ meV and $kT_{\parallel} \sim 0.03$ meV; the thermal cathode can be replaced by a photocathode electron source (Orlov *et al.* 2004), as described in §2*d*.

(b) *Vibrational and rotational excitation of the stored ion beam*

All the excited vibrational states of H_3^+ are sufficiently unstable against radiative decay that the ions will reach the vibrational ground state within storage times of about 2 s; this process was characterized by Coulomb explosion techniques on the extracted beam in independent measurements (Kreckel *et al.* 2002). Remarkably, the vibrational decay time of the lowest levels in the radiatively forbidden ν_1 mode, when compared with theoretical predictions, revealed a high degree of rotational excitation (Kreckel *et al.* 2002) with temperatures ranging up to 2000 K. Similar results were obtained in the analysis of DR products (Strasser *et al.* 2001). In fact, even high-lying rotational levels of H_3^+ ions performing planar rotation, corresponding to high K quantum numbers such as $(J,K)=(10,10)$, have lifetimes much exceeding the beam storage time, which leads to quasi-stationary high excitation in the stored beam if they are populated initially (Kreckel *et al.* 2004).

Both observations were made with H_3^+ ions produced in a hot electron-impact ion source. They motivated the development of colder ion sources pursued in recent years, together with studies of the isotopically asymmetrized ions D_2H^+ and H_2D^+ . The isotopically asymmetrized ions show much faster rotational cooling (Miller *et al.* 1989) and, unlike H_3^+ , have no ‘metastable’ rotational levels. Consequently, much lower rotational excitation was seen in fragment imaging measurements (Lammich *et al.* 2003*a*). The rotational temperature of stored beams could be reduced considerably by injecting them from a high-pressure hollow-cathode ion source cooled to 80 K by liquid nitrogen, built following the design from earlier H_3^+ experiments in Freiburg (Müller *et al.* 1999). The DR fragment imaging distributions with this source show a rotational-temperature upper limit of 1000 K, considerably lower than for the standard ion source (Altevogt 2003).

In order to probe rotational excitation in the stored ion beam with higher sensitivity, the time dependence of the DR rate coefficient at zero detuning velocity was measured at the TSR over long storage time intervals, ranging up to 80 s. In particular, varying the electron intensity and, in a later step, also the

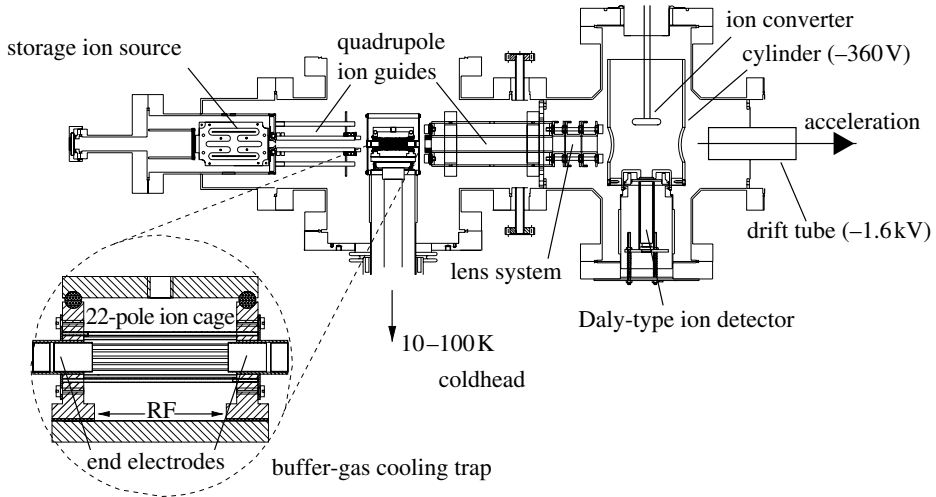


Figure 2. Set-up of the cryogenic ion injector trap coupled to the MeV RF high-energy accelerator feeding the TSR.

electron target energy, pump-probe-type experiments could be performed, trying to modify the rotational level populations in the stored ion beam. For D_2H^+ , these experiments yielded evidence for both considerable rotational dependence of the DR cross-section and rotational ion beam relaxation through cold electron interaction (Lammich *et al.* 2003b). Measurements with H_3^+ using the ‘warm’ source also showed variations of the DR rate coefficient, albeit with smaller amplitudes, as will be discussed in §4.

(c) The cryogenic ion injector trap at Test Storage Ring

For reliable internal cooling of H_3^+ ions before their transfer into the TSR, a cryogenic ion trap for buffer-gas cooling was realized, which can serve as an ion injector into the high-energy accelerator. The scheme of this injector is shown in figure 2. Its central part is a cylindrical 22-pole RF ion trap (Gerlich 1995) attached to a 10 K coldhead, where H_3^+ ions are confined within a steep-wall radial potential and additional axial potential wells at the trap ends. Here, the ions are cooled by He buffer gas (typical number density $(5-10) \times 10^{14} \text{ cm}^{-3}$) in an essentially field-free region; the free path length at this density (approx. 0.5 mm) is well below the trap dimensions. The ions are loaded in a pulse from the RF storage ion source (Teloy & Gerlich 1974) at *ca* 0.5 eV kinetic energy, stored for intervals between 1 and 100 ms, and after extraction from the trap transported slowly in a second quadrupole ion guide (range of investigated transport energies 0.5–20 eV) until their strong acceleration starts at much lower gas density (below 10^{11} cm^{-3}) at a distance of *ca* 18 cm from the trap. The system shown in figure 2 is installed on a high-voltage platform, so that the H_3^+ ions finally reach 12 keV for their injection into the high-energy accelerator. The temperature inside the cryogenic trap is $13 \pm 1 \text{ K}$ in operation. The trapped ion number, measured by acceleration of extracted ions onto a converter surface using the Daly (1960) scheme, ranged up to 2.5×10^6 , and for the beam transport into the TSR ion transmission factors of 40–50% were realized.

(d) Photocathode electron beam

The electron temperature, T_{\perp} , in the interaction region of an electron target can be reduced by magnetic expansion (Danared *et al.* 1994), but magnetic expansion factors appear to be limited to below 100 and the final electron temperature is proportional to their temperature at the electron beam formation and, hence, to the cathode bulk temperature. In order to improve T_{\perp} , a magnetically guided electron beam for high-resolution experiments was formed in the TSR electron target by a 3 mm diameter GaAs photocathode that replaced the usual thermoionic cathode (approx. 1200 K). This photocathode electron source is operated at a temperature of 100–120 K, being illuminated from the back by *ca* 0.5 W of infrared radiation from a GaAs laser diode to yield a space-charge-limited electron beam current of *ca* 250 μA . Details on the elaborate surface preparation methods, the emission properties and the operation of this electron source are given elsewhere (Pastuszka *et al.* 2000; Orlov *et al.* 2001, 2004). The electron beam is magnetically expanded (magnetic field ratio 20–40) to reduce the electron energy spread in the direction perpendicular to the magnetic guiding field. The transverse and the longitudinal electron temperatures in the co-moving frame of the accelerated photocathode electron beam were determined from a measurement of resonant structures in the HD^+ DR rate coefficient (Orlov *et al.* 2005) and found to be $kT_{\perp} = 500 \mu\text{eV}$ and $kT_{\parallel} = 25 \mu\text{eV}$, respectively, with estimated errors of $\pm 30\%$. An electron density of *ca* $4 \times 10^5 \text{ cm}^{-3}$ was obtained in the measurements. In a continuous operation, four photocathode samples are interchanged in a closed surface-processing cycle under vacuum, the typical operation time with a single sample being *ca* 10 h.

3. Energy-resolved dissociative recombination with cold H_3^+

(a) The low-energy energetic structure

Through the use of low-temperature collisional cooling, both the cryogenic buffer-gas cooling trap at the TSR and the molecular-beam expansion ion source by McCall *et al.* (2006) at the CRYRING are capable of producing H_3^+ ions with a rotational population essentially in the two lowest levels: $(J, K) = (1, 1)$ for *para*- H_3^+ (total nuclear spin $I = 1/2$), and $(1, 0)$ for *ortho*- H_3^+ ($I = 3/2$), energetically higher by 32.8 K (2.83 meV). Hence, it can be expected that storage-ring measurements with these injectors determine the rate coefficient for ions in these two levels only, provided that heating effects owing to either the beam transport and acceleration or the storage at high velocity in the magnetic ring are not significant.

Figure 3 shows the TSR results on the low-energy resonances of H_3^+ , obtained with the photocathode electron source ($kT_{\perp} = 500 \mu\text{eV}$) and the cryogenic buffer-gas cooling trap (Kreckel *et al.* 2005), in comparison with the CRYRING results (McCall *et al.* 2004) and theoretical predictions. The TSR data were checked against variations of experimental parameters in the cryogenic ion injector by measuring three spectra for trap storage times of 1, 10 and 100 ms; the data agreed within the statistical errors, where those for 10 and 100 ms carried the main statistics and, after averaging, were taken for the final result. Moreover, the recombination rates at zero detuning energy were recorded for different transport

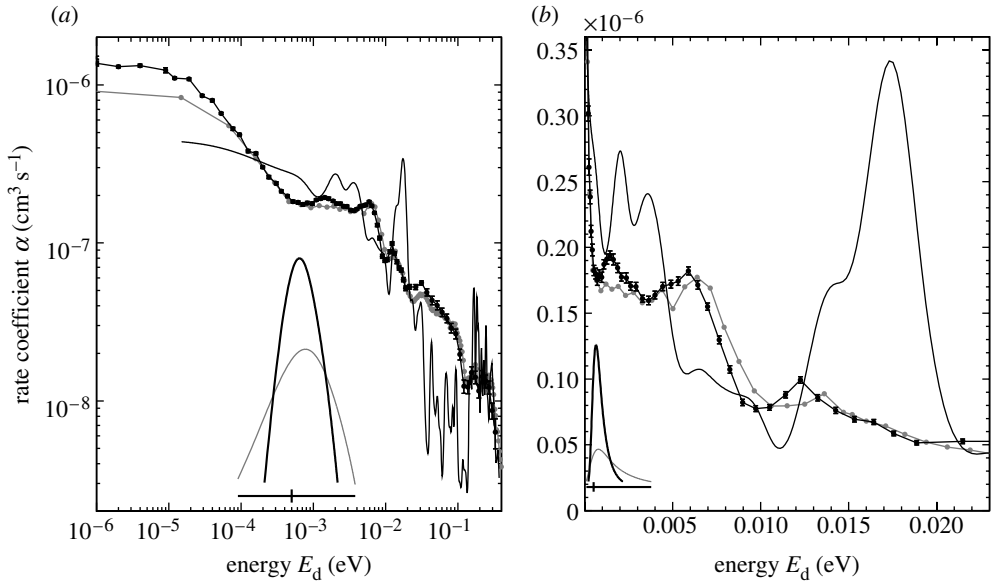


Figure 3. High-resolution DR rate coefficient of H_3^+ measured at the TSR (storage time in the ring 2–10 s) with the cryogenic ion injector trap and the photocathode electron source as a function of the detuning energy E_d (black dots), calibrated with the CRYRING data (McCall *et al.* 2004; grey dots) at the rotationally insensitive peak at $E_d = 10$ eV. Estimated uncertainty of the rate coefficient scale $\pm 20\%$. (a) Full low-energy part of the measurement; (b) enlargement of lowest energies. The electron energy distributions entering in the measured rate coefficients are shown in the insets for the TSR (black) and CRYRING (grey) parameters and for $E_d = 0.5$ meV. The theoretical prediction (continuous curve) uses the cross-sections of Kokkoouline & Greene (2003) for the two lowest H_3^+ levels with an *ortho*:*para* population ratio of 1 : 1, which includes toroidal averaging (Kokkoouline & Greene 2005) and is convoluted for $kT_{\perp} = 0.5$ meV and $kT_{\parallel} = 0.025$ meV.

energies in the second quadrupole ion guide (§2c), finding no significant variation between 0.5 and 20 eV; the measurements of figure 3 were performed at transport energies of 10–20 eV.

The results at the TSR and CRYRING turn out to be compatible with each other within *ca* 10%; small differences between the measurements at low energy (below 0.015 eV) can be explained by the lower electron temperature at the TSR (figure 3). The rate coefficient on the high-energy peak at 10 eV, experimentally shown to be independent on rotational excitation by Lammich *et al.* (2003b), is used to obtain an absolute calibration of the TSR data. The acceleration and storage parameters for both experiments are different in detail; for example, the acceleration is performed rapidly (within approx. 1 μ s) up to 5.3 MeV outside the ring at the TSR, while it is performed slowly (within approx. 2 s) from *ca* 0.1 to 12.1 MeV inside the ring at the CRYRING. Thus, the good agreement between the data largely excludes any significant population of higher excited H_3^+ levels through the different acceleration processes or (since the fields and their temporal sequence acting on a stored ion differ quantitatively) from the storage in the ring. It also appears highly unlikely that the observed DR rate originates from weakly populated H_3^+ levels which exhibit very large recombination rates, while low-lying rotational states have a small recombination rate. Such a situation, with

DR mainly from weakly populated vibrationally excited levels, while the ground-state DR is low, yielded results for the low-energy rate coefficient (and its ratio to the high-energy DR peak) clearly different from each other in two recent storage-ring experiments on ${}^3\text{He}{}^4\text{He}^+$, even at comparable storage times (Pedersen *et al.* 2005; Urbain *et al.* 2005).

Hence, the agreement of the datasets of the TSR and CRYRING presently makes them best suited for a detailed comparison with theoretical predictions on the DR of cold H_3^+ . In this comparison, less structure is found than theoretically predicted (in particular, at 0.01–0.2 eV). As explained previously, experimental evidence leaves little room for explaining the lack of structure and the missing rate between 0.03 and 0.1 eV by a superposition from a large number of rotational H_3^+ levels. The structures in the cross-section above 3 meV appear to be smeared by mutual superposition or natural broadening, as the energy resolution at the TSR would allow energetically more sharp structures to be seen readily in this region. The most narrow and only nearly resolution-limited structure is observed at about 1.4 meV (figure 3*b*). It is also remarkable that the two experiments consistently show a strong resonant contribution very close to the threshold, as represented by the rise at *ca* 500 μeV . This rise can be observed through the steep low-energy edge of the electron energy distribution (figure 3). In fact, the decreasing detuning energy E_d during a measurement shifts this steep edge over the resonance position; low-energy resonances then move into the range of the electron energy distribution, and thus contribute to the measured rate coefficient only at sufficiently low detuning energy E_d . In this way, resonances with energies E_r of $kT_{\parallel} \lesssim E_r \lesssim kT_{\perp}$ become visible in the data as shoulders. The observed rate coefficients consistently indicate a resonant structure starting below 50–100 μeV , but above the TSR limit of the longitudinal temperature $kT_{\parallel} = 25 \mu\text{eV}$.

In this context, it should be pointed out that the measurements at both rings took place in a longitudinal magnetic field, amounting to *ca* 570 mT for the TSR and *ca* 300 mT for the CRYRING (McCall *et al.* 2004). Electric stray fields in the interaction region are of the order of 1 V cm^{-1} . Moreover, it should be emphasized that the magnetic fields acting on the H_3^+ ions are time-dependent on the nanosecond scale. Hence, in spite of the good agreement between the measurements, it cannot be fully excluded at present that external, possibly, time-dependent external fields modify the experimental result.

Also transient electric fields are present at the entrance and the exit of the electron target and cooler, and they were found to produce an enhancement of the low-energy photorecombination rate of atomic ions in electron coolers (Gwinner *et al.* 2000; Hörndl *et al.* 2005). These effects also occur for bare ions and are not linked to resonances; they strongly increase with the ion charge, but they are still weak, in particular, for singly charged ions, where they enhance a rate coefficient of the order of only $10^{-11} \text{ cm}^3 \text{ s}^{-1}$ by *ca* 20% for D^+ (Gao *et al.* 1997). Also, the comparison of high-resolution storage-ring DR rate coefficients for the variety of experimentally studied species does not support any systematic low-energy enhancement for molecular ions, much unlike multicharged atomic ions. Hence, the observed results for H_3^+ DR seem to support a strong, narrow low-energy resonance very close to threshold.

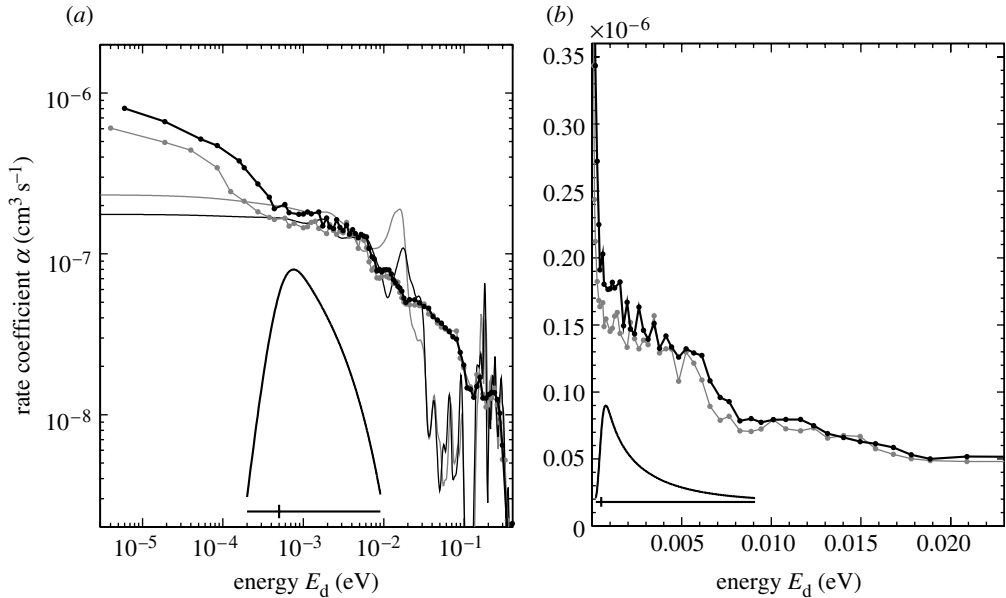


Figure 4. Energy-resolved DR rate coefficient for H_3^+ measured at the TSR using normal H_2 (grey dots) and $para$ - H_2 (black dots) in the cryogenic ion injector trap and employing the electron target with a thermoionic cathode (each dataset calibrated at the rotationally insensitive peak at $E_d=10$ eV peak as in figure 3). (a) Full low-energy part of the measurement; (b) enlargement of lowest energies. The electron energy distributions are shown for the parameters of this experiment (see text) and $E_d=0.5$ meV. The lines show the theoretical prediction with the cross-sections of Kokouline & Greene (2003) for the two lowest H_3^+ levels for an $ortho:para$ population ratio of 1 : 1 (grey) and for pure $para$ - H_3^+ (black), convoluted for $kT_{\perp}=4$ meV and $kT_{\parallel}=0.03$ meV.

(b) *Dependence on ortho- and para- H_3^+ populations*

The two lowest levels still populated in low-temperature, collisionally cooled H_3^+ ions are the states $(J,K)=(1,1)$ ($para$ - H_3^+ , $I=1/2$) and $(1,0)$ ($ortho$ - H_3^+ , $I=3/2$) 32.8 K higher. Considering the H_3^+ production in the ion injector (Cordonnier *et al.* 2000; Kreckel *et al.* 2005), the two levels should contribute with the high-temperature thermal population ratio ($ortho:para$) of 1 : 1, in figure 3, for the TSR data. Regarding the CRYRING experiment, McCall *et al.* (2004) assume that the observed relative populations of the $ortho$ and $para$ states represent the H_3^+ temperature, which for the quoted value of 31–33 K corresponds to a population ratio of 0.74. Hence, the $ortho:para$ ratio is roughly unity in both experiments, leading to the choice of 1 : 1 for this value in the theoretical data of figure 3.

The cryogenic ion injector trap at the TSR was used in an exploratory way to study the dependence of the rate coefficient on the population ratio of the two lowest H_3^+ levels. For this purpose, the gas fed into the ion source was changed from normal H_2 to $para$ - H_2 with an estimated purity of above 99%. This is expected to produce a relative enhancement of excited $para$ - H_3^+ states (Cordonnier *et al.* 2000), which are then cooled by He buffer gas without changing the spin symmetry abundancies. Figure 4 shows the DR rate coefficients observed when either normal H_2 or $para$ - H_2 was fed into the ion source (Kreckel *et al.* 2005). In contrast to figure 3, the

measurements were performed with the thermoionic electron source, yielding $kT_{\perp} = 4$ meV, $kT_{\parallel} = 0.03$ meV and an electron density of $ca\ 1 \times 10^7\text{ cm}^{-3}$. Differences in the DR rate coefficient are found below $ca\ 10$ meV, ranging up to $ca\ 25\%$, while the differences at higher energies are insignificant (below 10%).

We expect that the use of *para*-H₂ in the ion source leads to a reduction of the *ortho* : *para* ratio for H₃⁺ produced in the RF storage ion source (see §2c) at $ca\ 500$ K. It would be important to determine the actual *ortho* : *para* ratio for H₃⁺ in the ion trap or, best, directly inside the storage ring, but in spite of ongoing efforts such value is not available at present. However, the spectroscopic studies by Cordonnier *et al.* (2000) for various ion source types and operation modes found only reductions of the H₃⁺ *ortho* : *para* ratio, with values ranging from 0.8 down to 0.12, when normal H₂ was replaced by *para*-H₂; in fact, the production of H₃⁺ from electron-impact ionized *para*-H₂ first yields pure *para*-H₃⁺, but this species can be partly thermalized in the following (conversion to *ortho*-H₃⁺ being driven by hydrogen(H₂)-exchange reactions), where the thermalized fraction depended on the experimental parameters (Cordonnier *et al.* 2000). A further conversion of the H₃⁺ nuclear spin states in the cooling trap using He buffer gas is not expected (Oka 1973). Considering the energetics and selection rules, the (1,0) (*ortho*) state may be repopulated at 10 K by collisions with *ortho*-H₂ impurities; this possibility was reduced by using high He density (10^{15} cm^{-3}) and short storage time (approx. 0.5 ms). These arguments support that the *para*-H₂ measurement in figure 4 is, in fact, performed at a comparatively increased abundance of *para*-H₃⁺ in the stored ion beam; the size of this increase, however, cannot be given at this stage.

Energy shifts by the interaction of the molecular magnetic moment with the external magnetic fields are small (on the level of below 10^{-3} K for fields of 1 T) compared to the spacing between the *ortho*- and *para*-H₃⁺ levels. Nevertheless, the magnetic fields acting periodically on the stored ions in the bending fields amount to $ca\ 0.5$ T for 5.3 MeV H₃⁺ in the TSR, with rise and fall times of $ca\ 10$ ns and dwell times of $ca\ 50$ ns, respectively. While a strong modification of the *ortho* : *para* ratio through induced transitions in these fields does not appear probable and is not so far taken into account, further considerations and a direct *in situ* measurement of the level populations in the stored beam are desirable in the future.

Even in view of the limited information on the H₃⁺ *ortho* : *para* ratio in the stored beam, the observed rate coefficients of figure 4 appear to behave differently from the theoretical predictions, the low-energy rate coefficient being enhanced for *para*-H₂ ion source gas and other predicted strong *ortho*-*para* differences being absent.

4. Rotational cooling and heating of H₃⁺ in the storage ring

Studies on internal excitation of stored H₃⁺ ions were performed in the TSR during about two years preceding the use of the cryogenic injector trap. Using long storage times up to $ca\ 80$ s, these experiments observed temporal changes of the rotational excitation for the isotopically modified species of both D₂H⁺ (Lammich *et al.* 2003b) and H₃⁺ (Lammich *et al.* 2005), using a ‘hot’ electron-impact ion source and the ‘warm’ ion source, respectively (§2b). The absolute rate coefficient for D₂H⁺ (Lammich *et al.* 2003b) below $ca\ 0.1$ eV was found to decrease by a factor of up to ca

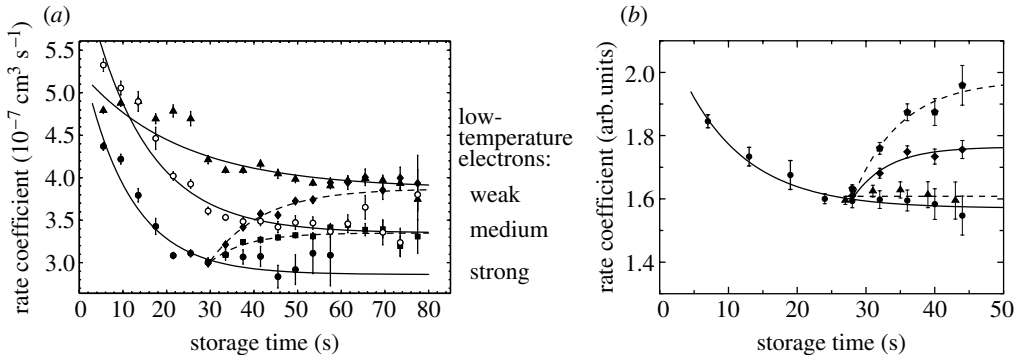


Figure 5. DR rate coefficient at matched beam velocities ($E_d=0$) as a function of the storage time in the TSR following injection (TSR electron cooler with $kT_{\perp}=12$ meV, $kT_{\parallel}=0.07$ meV and electron density of $1.1 \times 10^7 \text{ cm}^{-3}$ unless otherwise stated). Lines are to guide the eye. (a) D_2H^+ : full lines, low-temperature electrons with interaction times relative to the total storage time of 0.45% (triangles) and 2.48% (full circles), as well as with 2.48% but half electron density (open circles); broken lines, cooling cycle reduced to 1.35 (squares) and 0.45% (diamonds) at full electron density. Estimated uncertainty of the rate coefficient $\pm 30\%$. (b) H_3^+ : full lines, interaction time of 2.2% (circles) and for reduction to 0.89% at 28 s (diamonds); broken lines, interaction time of 2.2% with low-temperature electrons plus energetic pump electrons (electron target) with 2.5% of interaction time above 28 s, pump energy 10 eV (triangles) and 0.116 eV (pentagons). One arbitrary unit corresponds to a rate coefficient of $1 \times 10^{-7} \text{ cm}^3 \text{ s}^{-1}$ with $\pm 50\%$ accuracy.

1.65 for long storage times (30–60 s) as compared with short ones (5–15 s), while the high-energy rate coefficient with the well-known peak at 10 eV remained constant. This reflects a slow decrease in the low-energy rate coefficient with a rate of $(10 \text{ s})^{-1}$ or lower. As the vibrational cooling of D_2H^+ and H_3^+ ions proceeds with much higher decay rates above $(2 \text{ s})^{-1}$, slower variations of the rate coefficient can only be explained by changes of the relative *rotational* level populations in the stored ion beam. Hence, these measurements prove the rotational dependence of the low-energy DR rate coefficient and simultaneously provide us with a method of monitoring the time variation of rotational populations.

The time-dependent data for D_2H^+ (figure 5a; Lammich *et al.* 2003b) show a relatively strong decrease in the rate coefficient ratio (up to a factor of 1.8) with storage time. When the electron interaction is reduced to just the minimum necessary for monitoring the DR rate, the decrease becomes slower, but settles at a time dependence representing the spontaneous radiative relaxation of the lowest rotational levels. This shows the trend of the low-energy DR rate coefficient to decrease with decreasing rotational excitation, and yields its value for thermalized rotational populations near room temperature. Furthermore, stronger interaction with low-temperature electrons is shown to yield even faster reductions of the DR rate coefficient and smaller stationary values at long storage time. As the electron temperature in the co-propagating reference frame amounts to *ca* 140 K, equilibrium rotational temperatures below room temperature are feasible thermodynamically and, indeed, seem to be realized.

In the interpretation of the electron-induced cooling process, it must be taken into account that the DR of D_2H^+ and H_3^+ in the overlapping electron beam represents a significant beam loss process. For a relative interaction time with

electrons (referred to the total storage time) of typically 2.5% ('maximum cooling'), the electron density of $1.1 \times 10^7 \text{ cm}^{-3}$ and a DR rate coefficient of $3 \times 10^{-7} \text{ cm}^3 \text{ s}^{-1}$, the total DR loss rate is close to $(10 \text{ s})^{-1}$, near the observed rates of decrease for the low-energy DR rate coefficient. Hence, with large *differences* between the rate coefficients for individual rotational levels, rotational cooling by differential depletion of rotational levels through DR is possible. On the other hand, the observed reductions can also be owing to direct electron-induced cooling (SEC), not linked with ion loss. As the observed cooling rates turn out to be of similar size as the ion loss rates, the effects of SEC and DR could not so far be distinguished from each other, although this will be attempted in the future.

As a second step, it is interesting to consider the same type of measurements for H_3^+ . Such measurements were performed with the liquid nitrogen-cooled hollow-cathode ion source described previously, yielding a 'warm' rotational level population (presumably roughly up to $J=4$) with all radiative lifetimes above 10^3 s . The time-dependent data for H_3^+ (figure 5*b*; Lammich *et al.* 2005) do show a decrease in the monitored low-energy DR rate coefficient ratio, but only by a factor of about 1.2 with a decay rate of *ca* $(15 \text{ s})^{-1}$. Depending on the experimental conditions, in particular the ion source parameters, also stronger initial decreases up to a factor of *ca* 1.5 were found with strong electron cooling. Reducing the electron cooling intensity to *ca* 0.4 of its initial value once the DR rate coefficient has levelled off makes it grow again, which indicates the presence of a rotational repopulation process working against the low-temperature electrons and proceeding with a rate of *ca* $(6 \text{ s})^{-1}$.

Also here, the observed time constants are in the range of the DR loss rate, which makes differential depletion of more strongly recombining levels possible in the case of large differences between the rate coefficients. Moreover, these data carry no intrinsic indication on the trend of DR rates with increasing rotational excitation, in contrast to the blackbody relaxation seen in the D_2H^+ data. Hence, the observed decrease for H_3^+ could basically also be caused by the preferential depletion of *low* rotational states if (at vanishing electron velocity detuning) they recombine more strongly than higher levels, giving effective heating.

In a final step, the excitation induced by energetic electrons was studied. Here, once the DR rate coefficient had levelled off after the initial decrease, a second, energy variable electron beam was applied in the electron target, in addition to the cooler which continued to probe the low-energy DR. The energetic electrons (density approx. $2 \times 10^7 \text{ cm}^{-3}$) caused an increase in the low-energy DR rate coefficient up to a new stationary value shown in figure 6 as a function of the applied electron energy. The electron-induced population of more strongly recombining levels appears to be strongest at *ca* 0.1 eV and then slowly decreases again. From the rise times in figure 5*b*, it follows that the excited levels do not decay faster than *ca* $(6 \text{ s})^{-1}$, which is the case only for rotational levels. Consequently, no significant structure is seen at the vibrational excitation thresholds, the lowest of which is indicated in figure 6. Below 0.1 eV, the final rate coefficient was found to decrease again, but these data are experimentally uncertain as the high-density electron beam of the target shifted the ion velocity, thus reducing the rate coefficient, at low pump energy (below 50 meV). Towards 10 eV, the electron pumping effect becomes small again, which indicates that

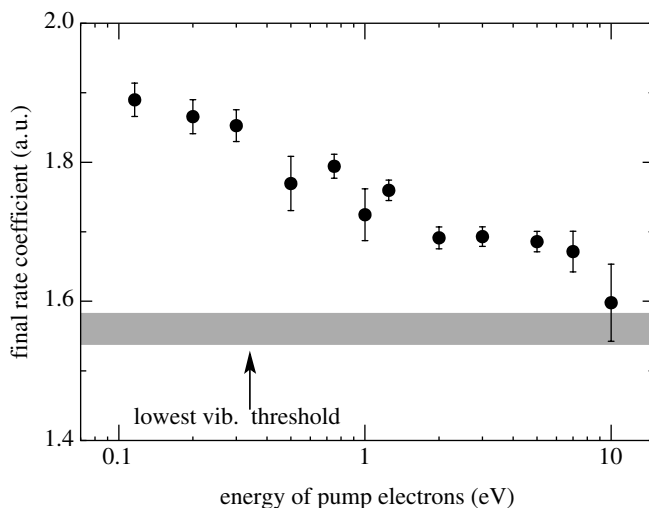


Figure 6. The final rate coefficient reached in figure 5 (average of 37–47 s) as a function of the pump electron energy. The pump electron density was $ca\ 2 \times 10^7\text{ cm}^{-3}$, decreasing by $ca\ 20\%$ between 0.1 and 10 eV. Low-temperature electrons are always present in addition at 2.2% of the interaction time; only the final rate coefficient reached with low-temperature electrons is indicated by the shaded band. Vibrational excitation is possible above the energy indicated by the arrow. Data points below 0.1 eV exist (Lammich *et al.* 2005), but are experimentally uncertain.

electrons of this energy, intermittently applied in all measurements for probing the DR rate coefficient ratio, do not significantly modify the stationary low-energy DR rate coefficient in the measurements of §2.

The data of figure 6 can very likely be interpreted as a rotational electron-impact excitation curve for H_3^+ , pertaining, however, to levels whose initial rotation is not known. Taking this viewpoint, it would appear also for H_3^+ that more energetic rotational levels, as a trend, have higher low-energy DR rate coefficients, so that the decrease in figure 5b is linked to rotational cooling also for this species. The rotational repopulation process working against the cooling by low-temperature electrons, as described previously, most probably represents heating in the residual gas. The data of figure 5b can be used to estimate the relative effect of both heating processes on the low-energy DR rate. For the residual gas heating, the relative increase in this rate at strong cooling is estimated from its rise when the electron interaction time is reduced by a factor of $r=0.89/2.2=0.4$; since the asymptotic level is inversely proportional to the electron cooling rate, this should represent $(1/r-1)$ times the increase at strong cooling, so that this increase itself amounts to $0.18/1.5=0.12$ arb. unit, or 8%. The corresponding fraction of excited H_3^+ species in the ring cannot be determined without knowing the DR rate coefficient of this level as compared to others; however, the level strongly reacts to electrons as the stationary level is reached fast and the state thus seems to show rapid electron cooling, $ca\ (6\text{ s})^{-1}$. This suggests that its low-energy DR rate is not smaller, rather larger than on average, indicating excited-state abundances from rest-gas heating on at most the 10% level.

Therefore, the heating measurements for a ‘warm’ H_3^+ beam discussed here indicate a small fraction of excited ions in a stored beam, remaining limited to 10% at most, through rotational excitation in the residual gas. This supports the conclusion that the cold H_3^+ measurements discussed previously (§3) are only insignificantly influenced by excited rotational states above $J=1$. Nevertheless, with suitable *in situ* diagnostic tools becoming available, it would be desirable to search more sensitively for excited-state contributions in further more detailed experimental studies.

5. Conclusions

Studies of the internal state of H_3^+ ions in an ion storage ring by Coulomb explosion, showing vibrational relaxation, have been complemented by time-dependent DR measurements sensitive to rotational excitations, using storage times up to 80 s. Clear time variations of the low-energy DR rate coefficients are observed, showing a decrease by up to a factor of 2 for rotationally hot ions under the effect of electrons at temperatures of *ca* 140 K, as well as increases in the 10% range both by rest-gas interactions and energetic electron impact. Cold ion sources for H_3^+ ions have been introduced at two storage-ring facilities and show a consistent set of resonant structures at low energy, which could be resolved down to $E_d \sim 1$ meV in the measurements at the TSR applying a photocathode electron beam. The agreement of the energy-dependent rate coefficients from different storage-ring experiments gives a strong evidence that the observed structures arise from cold H_3^+ ions in the two lowest rotational levels. However, these structures deviate in their shape and in their response to nuclear spin symmetry changes from the recent theoretical predictions of Kokoouline & Greene (2003), which is the more remarkable as this approach well predicts the thermally averaged rate coefficient and has greatly improved the understanding of the H_3^+ recombination process. Future experiments would greatly profit from improved diagnostic possibilities for the population of rotational levels in the stored H_3^+ . This would make it possible to identify the DR contributions of individual rotational levels, to find even small contributions in the observed energetic structure from excited rotational states and to measure electron-induced rotational excitation and cooling rates.

We thank C. H. Greene and V. Kokoouline for their helpful discussions and for making their state-specific DR cross-sections available to us in numerical form. This work has been funded in part by the German Israel Foundation for Scientific Research (GIF) under contract I-707-55.7/2001 and by the Grant Agency of the Czech Republic under GACR 205/05/0390 and 202/05/P095.

References

- Al-Khalili, A. *et al.* 2002 Absolute high-resolution rate coefficients for dissociative recombination of electrons with HD^+ : comparison of results from three heavy-ion storage rings. *Phys. Rev. A* **68**, 042702. (doi:10.1103/PhysRevA.68.042702)
- Altevogt, S. 2003 Production of rotationally cold H_3^+ ions with a hollow cathode ion source. Diploma thesis, University of Heidelberg.
- Cordonnier, M., Uy, D., Dickson, R. M., Kerr, K. E., Zhang, Y. & Oka, T. 2000 Selection rules for nuclear spin modifications in ion-neutral reactions involving H_3^+ . *J. Chem. Phys.* **113**, 3181–3193. (doi:10.1063/1.1285852)

- Daly, N. R. 1960 Scintillation type mass spectrometer ion detector. *Rev. Sci. Instrum.* **31**, 264–267. (doi:10.1063/1.1716953)
- Danared, H. *et al.* 1994 Electron cooling with an ultracold electron beam. *Phys. Rev. Lett.* **72**, 3775–3778. (doi:10.1103/PhysRevLett.72.3775)
- Faure, A. & Tennyson, J. 2003 Rate coefficients for electron-impact rotational excitation of H_3^+ . *Mon. Not. R. Astron. Soc.* **340**, 468–472. (doi:10.1046/j.1365-8711.2003.06306.x)
- Gao, H., Schuch, R., Zong, W., Justiniano, E., DeWitt, D. R., Lebius, H. & Spies, W. 1997 Energy and charge dependence of the rate of electron-ion recombination in cold magnetized plasmas. *J. Phys. B: At. Mol. Opt. Phys.* **30**, L499–L506. (doi:10.1088/0953-4075/30/14/003)
- Gerlich, D. 1995 Ion-neutral collisions in a 22-pole trap at very low energies. *Phys. Scr.* **T59**, 256–263.
- Gwinner, G. *et al.* 2000 Influence of magnetic fields on electron-ion recombination at very low energies. *Phys. Rev. Lett.* **84**, 4822–4825. (doi:10.1103/PhysRevLett.84.4822)
- Hörndl, M., Yoshida, S., Wolf, A., Gwinner, G. & Burgdörfer, J. 2005 Enhancement of low energy electron-ion recombination in a magnetic field: influence of transient field effects. *Phys. Rev. Lett.* **95**, 243 201. (doi:10.1103/PhysRevLett.95.243201)
- Jaeschke, E. *et al.* 1990 First electron cooling of heavy ions at the new Heidelberg storage ring TSR. *Part. Accel.* **32-33**, 1539–1546.
- Kokouline, V. & Greene, C. H. 2003 Unified theoretical treatment of dissociative recombination of D-3h triatomic ions: application to H_3^+ and D_3^+ . *Phys. Rev. A* **68**, 012 703. (doi:10.1103/PhysRevA.68.012703)
- Kokouline, V. & Greene, C. H. 2005 Theoretical study of dissociative recombination of C_{2v} triatomic ions: application to H_2D^+ and D_2H^+ . *Phys. Rev. A* **72**, 022 712. (doi:10.1103/PhysRevA.72.022712)
- Kreckel, H. *et al.* 2002 Vibrational and rotational cooling of H_3^+ . *Phys. Rev. A* **66**, 052 509. (doi:10.1103/PhysRevA.66.052509)
- Kreckel, H., Tennyson, J., Schwalm, D., Zajfman, D. & Wolf, A. 2004 Rovibrational relaxation model for H_3^+ . *New J. Phys.* **6**, 515. (doi:10.1088/1367-2630/6/1/151)
- Kreckel, H. *et al.* 2005 High resolution dissociative recombination of cold H_3^+ and first evidence for nuclear spin effects. *Phys. Rev. Lett.* **95**, 263 201. (doi:10.1103/PhysRevLett.95.263201)
- Lammich, L., Kreckel, H., Krohn, S., Lange, M., Schwalm, D., Strasser, D., Wolf, A. & Zajfman, D. 2003a Breakup dynamics in the dissociative recombination of H_3^+ and its isotopomers. *Rad. Phys. Chem.* **68**, 175–179. (doi:10.1016/S0969-806X(03)00276-7)
- Lammich, L. *et al.* 2003b Evidence for subthermal rotational populations in stored molecular ions through state-dependent dissociative recombination. *Phys. Rev. Lett.* **91**, 143 201. (doi:10.1103/PhysRevLett.91.143201)
- Lammich, L. *et al.* 2005 DR rate measurements using stored beams of H_3^+ and its isotopomers. *J. Phys.: Conf. Ser.* **4**, 98–103. (doi:10.1088/1742-6596/4/1/013)
- Larsson, M. 1997 Dissociative recombination with ion storage rings. *Ann. Rev. Phys. Chem.* **48**, 151–179. (doi:10.1146/annurev.physchem.48.1.151)
- Larsson, M. 2000 Dissociative electron-ion recombination studies using ion synchrotrons. In *Photoionization and photodetachment*, vol. 10, part II (ed. C. Y. Ng) *Advanced series in physical chemistry*, pp. 693–747. Singapore: World Scientific.
- LePetit, F., Roueff, E. & Herbst, E. 2004 H_3^+ and other species in the diffuse cloud towards ζ Persei: a new detailed model. *Astron. Astrophys.* **417**, 993–1002. (doi:10.1051/0004-6361:20035629)
- McCall, B. J. *et al.* 2003 An enhanced cosmic-ray flux towards ζ Persei inferred from a laboratory study of the H_3^+ recombination rate. *Nature* **422**, 500–502. (doi:10.1038/nature01498)
- McCall, B. J. *et al.* 2004 Dissociative recombination of rotationally cold H_3^+ . *Phys. Rev. A* **70**, 052 716. (doi:10.1103/PhysRevA.70.052716)
- McCall, B. J. 2006 Dissociative recombination of cold H_3^+ and its interstellar implications. *Phil. Trans. R. Soc. A* **364**, 2953–2963. (doi:10.1098/rsta.2006.1876)
- Miller, S., Tennyson, J. & Sutcliffe, B. T. 1989 First principles calculation of rotational and ro-vibrational line strengths. Spectra for H_2D^+ and D_2H^+ . *Mol. Phys.* **66**, 429–456. (doi:10.1080/002689789001100211)

- Müller, U., Eckert, T., Braun, M. & Helm, H. 1999 Fragment correlation in the three-body breakup of triatomic hydrogen. *Phys. Rev. Lett.* **83**, 2718–2721.
- Ngassam, V., Motapon, O., Florescu, A., Pichl, L., Schneider, I. F. & Suzor-Weiner, A. 2003 Vibrational relaxation and dissociative recombination of H_3^+ induced by slow electrons. *Phys. Rev. A* **68**, 032 704. (doi:10.1103/PhysRevA.68.032704)
- Oka, T. 1973 Collision-induced transitions between rotational levels. *Adv. At. Mol. Phys.* **9**, 127–206.
- Orlov, D. A., Hoppe, M., Weigel, U., Schwalm, D., Terekhov, A. S. & Wolf, A. 2001 Energy distributions of electrons emitted from GaAs(Cs,O). *Appl. Phys. Lett.* **78**, 2721–2723. (doi:10.1063/1.1368376)
- Orlov, D. A., Sprenger, F., Lestinsky, M., Weigel, U., Terekhov, A. S., Schwalm, D. & Wolf, A. 2005 Photocathodes as electron sources for high resolution merged beam experiments. *J. Phys.: Conf. Ser.* **4**, 290–295. (doi:10.1088/1742-6596/4/1/045)
- Orlov, D. A., Weigel, U., Schwalm, D., Terekhov, A. S. & Wolf, A. 2004 Ultra cold electron source with a GaAs-photocathode. *Nucl. Instrum. Methods A* **532**, 418–421. (doi:10.1016/j.nima.2004.06.048)
- Pastuszka, S., Hoppe, M., Kratzmann, D., Schwalm, D., Wolf, A., Jaroshevich, A. S., Kosolobov, S. N., Orlov, D. A. & Terekhov, A. S. 2000 Preparation and performance of transmission-mode GaAs-photocathodes as sources for cold DC electron beams. *J. Appl. Phys.* **88**, 6788–6800. (doi:10.1063/1.1311307)
- Pedersen, H. B. *et al.* 2005 Dissociative recombination and low-energy inelastic electron collisions of the helium dimer ion. *Phys. Rev. A* **72**, 012 712. (doi:10.1103/PhysRevA.72.012712)
- Poth, H. 1990 Electron cooling: theory, experiment, application. *Phys. Rep.* **196**, 135–297. (doi:10.1016/0370-1573(90)90040-9)
- Sprenger, F., Lestinsky, M., Orlov, D., Schwalm, D. & Wolf, A. 2004 The high resolution electron-ion collision facility at TSR. *Nucl. Instrum. Methods A* **532**, 298–302. (doi:10.1016/j.nima.2004.06.058)
- Strasser, D., Lammich, L., Kreckel, H., Krohn, S., Lange, M., Naaman, A., Schwalm, D., Wolf, A. & Zajfman, D. 2002*b* Breakup dynamics and the isotope effect in H_3^+ and D_3^+ dissociative recombination. *Phys. Rev. A* **66**, 032 719. (doi:10.1103/PhysRevA.66.032719)
- Strasser, D., Lammich, L., Kreckel, H., Lange, M., Krohn, S., Schwalm, D., Wolf, A. & Zajfman, D. 2004 Breakup dynamics and isotope effects in D_2H^+ and H_2D^+ dissociative recombination. *Phys. Rev. A* **69**, 064 702. (doi:10.1103/PhysRevA.69.064702)
- Strasser, D. *et al.* 2001 Two- and three-body kinematical correlation in the dissociative recombination of H_3^+ . *Phys. Rev. Lett.* **86**, 779–782. (doi:10.1103/PhysRevLett.86.779)
- Strasser, D., Levin, J., Pedersen, H. B., Heber, O., Schwalm, D., Wolf, A. & Zajfman, D. 2002*a* Branching ratios in the dissociative recombination of polyatomic ions: the H_3^+ case. *Phys. Rev. A* **65**, 010702(R).
- Teloy, E. & Gerlich, D. 1974 Integral cross sections for ion-molecule reactions. I. The guided beam technique. *Chem. Phys.* **4**, 417–427. (doi:10.1016/0301-0104(74)85008-1)
- Urbain, X., Djuric, N., Safvan, C. P., Jensen, M. J., Pedersen, H. B., Sogaard, L. V. & Andersen, L. H. 2005 Storage ring study of the dissociative recombination of He_2^+ . *J. Phys. B: At. Mol. Opt. Phys.* **38**, 43–50. (doi:10.1088/0953-4075/38/1/004)
- Wolf, A. 1999 Heavy-ion storage rings. In *Atomic physics with highly charged ions* (ed. H. F. Beyer & V. P. Shevelko), pp. 3–29. Berlin, Germany: Springer.
- Wolf, A., Krohn, S., Kreckel, H., Lammich, L., Lange, M., Strasser, D., Grieser, M., Schwalm, D. & Zajfman, D. 2004 Cooling of molecular ion beams. *Nucl. Instrum. Methods A* **532**, 69–78. (doi:10.1016/j.nima.2004.06.031)

Discussion

R. THOMAS (*Stockholm University, Sweden*). You have measured the low-energy DR rate coefficients after electron and residual gas excitation of the H_3^+ ions. Once that excited, stored H_3^+ ions are obtained this way, would it be possible to

perform also other cross-section measurements on them in order to understand their nature and properties?

A. WOLF. An extension of the pump–probe type studies described here would be promising in order to access excited-state properties. One could concentrate on strong features in the DR cross-section, such as the high-energy peak occurring at *ca* 7 eV; measurements of this type are demanding owing to the small intensity of the H_3^+ beam left after its long storage, but should become feasible if processes with high enough cross-sections are chosen.

R. E. CONTINETTI (*University of California, San Diego, USA*). I recall that with GaAs photocathodes, one can form spin-polarized electron beams. Is there any net electron-spin polarization in your present configuration, or could you make use of this in future studies to measure, say, electron-spin dependent differential cross-sections for dissociative recombination?

A. WOLF. In the present operation, an electron-spin polarization does not exist at our photocathode, but this is one of our options for further developments. A polarization longitudinal to the electron beam direction can be implemented in our set-up in a straightforward manner using the well-introduced technology of a strained GaAs crystal and circularly polarized illumination. Spin-related asymmetries in the differential cross-section for dissociative recombination could, for suitable molecular species, lead to differences in the fragment geometry between the forward and the backward directions along the beam detectable by the three-dimensional fragment imaging implemented at the TSR.

M. LARSSON (*Stockholm University, Sweden*). The rise of the H_3^+ dissociative recombination rate coefficient at electron-impact energies below 0.3 meV is consistent between CRYRING and TSR, but different from the theoretical calculation. This raises the question if it is possible that theory missed a resonance at *ca* 0.1 meV or below.

C. H. GREENE (*University of Colorado, Boulder, USA*). It is certainly possible and even expected that some of the calculated resonance positions in our theoretical description should be in error by more than 0.1 meV. Such errors can be caused, for instance, by the energy dependence of the quantum defect information, which leads to errors much larger than 0.1 meV for perturbers of low principal quantum number. Detailed laser spectroscopy, for instance, of the type H. Helm's group has carried out, might in principle allow us to test the accuracy of the resonance positions, and it might also suggest how to improve the calculation.